



*Cent. Eur. J. Energ. Mater.* 2021, 18(2): 271-286; DOI 10.22211/cejem/139576

Article is available in PDF-format, in colour, at:

<https://ipo.lukasiewicz.gov.pl/wydawnictwa/cejem-woluminy/vol-18-nr-2/>



Article is available under the Creative Commons Attribution-Noncommercial-NoDerivs 3.0 license CC BY-NC-ND 3.0.

*Research paper*

## A Comparative Numerical and Experimental Study of Light Weight Materials for Neutralizing Explosive Reactive Armour

Khalid Naeem<sup>1,\*</sup>, Arshad Hussain<sup>1</sup>, Abdul Qadeer Malik<sup>1</sup>,  
Shakeel Abbas<sup>2</sup>, Iftikhar Ahmad<sup>1</sup>, Sarah Farrukh<sup>1</sup>

<sup>1</sup> School of Chemicals and Material Engineering, NUST, Pakistan

<sup>2</sup> Al-Technique Corporation of Pakistan, Pakistan

\* E-mail: [khalid.phd@scme.nust.edu.pk](mailto:khalid.phd@scme.nust.edu.pk)

**Abstract:** Explosive reactive armour (ERA) consists of an explosive sandwiched between two metal plates fitted on armoured vehicles to enhance their protection. To defeat an ERA mounted vehicle, its ERA must be neutralized first. A precursor fitted in a TANDEM warhead is used for this purpose in two modes. One is to detonate the ERA and the other is without detonation. This paper presents work performed on the ability of light-weight materials to neutralize the Kontakt-5 ERA without detonation. The precursor performing in this manner is known as a non-initiating precursor (NIP).

Eight experiments were performed with aluminium, Teflon<sup>®</sup> and perspex as liners, against Kontakt-5 ERAs at about 90° and 30° inclination. In five of these experiments, the ERA did not detonate, however in three experiments it did detonate. In all of the experiments the precursor over-performed, producing a prominent hole in the target larger than that predicted by simulation. The over-performance was balanced by decreasing the angle of attack.

These experiments demonstrated that an NIP depends strongly upon the ERA as well as on the angle of attack. The overall conclusion from this work is that an NIP is a promising technique to defeat a specific ERA without detonation.

**Keywords:** simulation, explosive reactive armour, Kontakt-5, non-initiating precursor, tandem

## 1 Introduction

Explosive reactive armour (ERA) is a device retrofitted on tanks or other combat vehicles for their protection. It consists of an explosive sandwiched between two metal plates [1]. A Tandem warhead is used to defeat ERA mounted vehicles. Conventionally the precursor of the Tandem detonates the ERA. Such a warhead is cumbersome, lengthy, needs an extended time delay and exhibits fragmentation and back-blast effects. These limitations can be minimised by neutralizing the ERA without initiation. The precursor utilized for this purpose is known as a non-initiating precursor (NIP). In order to design a NIP, the “ $v^2d$ ” criterion introduced by Held [2] was strictly followed in the simulations, where  $v$  and  $d$  are the tip velocity and diameter of the jet, respectively. This criterion for a few explosives is shown in Figure 1. Only those liners which passed the “ $v^2d$ ” criterion were selected for fabrication.

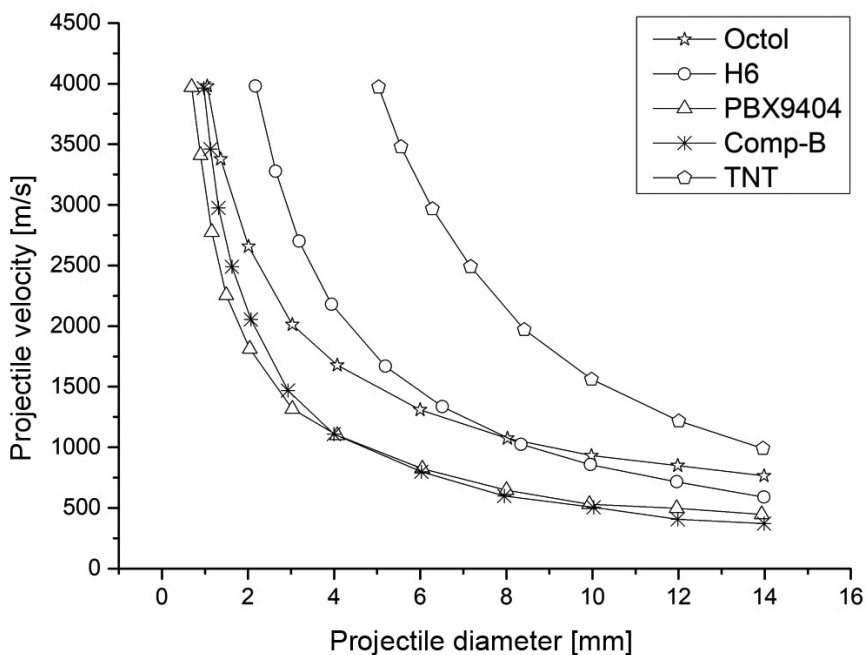


**Figure 1** The “ $v^2d$ ” criterion for some explosives [2]

This paper includes a brief review of related research, the simulation techniques conducted by Autodyn and LS Dyna, and the experimental results. Based on the simulations, explosively formed projectiles (EFPs) were designed,

assembled and tested against Kontakt-5 at two angles of attack and the results are displayed in pictorial form.

Numerical investigation of the detonation of a double reactive cassette, when impacted with different nose-shaped projectiles, was carried out by Shin and Lee [3]. “M” and “W” type configurations of EFPs were studied by Wiśniewski and Podgórzak [4] to neutralize ERAs, and it was found that an M-type liner can perforate the first generation ERA without detonation. The interaction process between the ERA and the shaped charge was studied by Held, who concluded that an ERA can be defeated by a high precision-shaped charge, which also produces more penetration behind the ERA than large angle shaped charges [5]. Momentum theory for the flying ERA plates was also given by Held [6]. In some cases two ERAs were mounted one upon the other, and work on the sensitivity of the explosive for a single and double-layered ERA was also carried out by Wiśniewski [7]. The first generation ERA, having designation 3-3-3, was tested in the research carried out by Helte and Lundgren [8]. The numbers 3-3-3 represent the thicknesses of the ERA front plate, the explosive sandwich and the backplate, respectively. In order to successfully design an ERA, various explosives were tested within the two flying metal plates. In such an attempt, a nitrocellulose and cellulose composite was tested theoretically and experimentally by Trzciński *et al.* [9]. A theoretical model for an ERA interaction with a shaped charge jet was introduced by Micković *et al.* [10]. The movement of the forward and rearward going plates of the ERA were studied by NERA code and were found to be in agreement with experimental data. The effect of the front plate thickness of the ERA against the EFP was studied by Rasheed *et al.* [11]. The initiation criteria for an explosive by steel, tungsten, aluminium and copper of varying diameters is given in the work of Bouvenot [12]. Jet formation and its damage was investigated for low density materials *i.e.* lucite, floatglass and Plexiglas by Ding *et al.* [13] using simulation. The effects of the ERA cover plate and its thickness when the EFP interacts with it was studied by Rasheed *et al.* [14]. It was concluded that the decrease in penetration is directly proportional to the thickness of the cover plate. The current paper includes simulation and experimental research conducted to design an NIP for Kontakt-5 ERA. This will provide guidelines for research into the design of NIPs against any kind of ERA.

## 2 Material and Methods

### 2.1 Autodyn simulations

Simulation is one of the cheapest and quickest means to assess the results. Ansys Autodyn and LS Dyna were used to design the NIP. Simulations were carried out in the light of the “ $v^2d$ ” criterion. Autodyn 2-D simulation with axial symmetry was employed to minimize the computational efforts and to decrease the run time. The units utilized in the simulations were millimetre, milligram and millisecond for length, mass and time, respectively. Tetryl was used as the booster and Comp-B as the main charge for the EFP. Tetryl and Comp-B were modelled by the Jones-Wilkins-Lee (JWL) equation of state [15] defined by Equation 1:

$$p = A \left(1 - \frac{\omega}{R_1 v}\right) \exp(-R_1 v) + B \left(1 - \frac{\omega}{R_2 v}\right) \exp(-R_2 v) + \frac{\omega E}{v} \quad (1)$$

where the terms  $p$ ,  $E$  and  $v$  are the detonation pressure, internal energy per unit volume and relative volume, respectively, whereas the terms  $A$ ,  $B$ ,  $R_1$ ,  $R_2$  and  $\omega$  are constants. The JWL parameters for the two explosives are tabulated in Table 1.

**Table 1** JWL parameters [6]

Material	$p$ [k Pa]	$E$ [kJ/m <sup>3</sup> ]	$A$	$B$	$R_1$	$R_2$	$\omega$	Density [g/cm <sup>3</sup> ]	D [m/s]
Tetryl	2.85e7	8.2e6	5.868e8	1.067e7	4.4	1.2	0.275	1.73	7.91e3
Comp-B	2.95e7	8.5e6	5.242e8	7.67e7	4.2	1.1	0.34	1.717	7.98e3

The shock equation of state utilized for materials other than the explosives is given by Equation 2:

$$v_s = c_1 + m v_p \quad (2)$$

where  $v_s$ ,  $c_1$ ,  $m$  and  $v_p$  are the shock wave velocity, particle velocity, a constant and the slope, respectively. The constant is the “Y-axis” intercept of the graph between  $v_s$  and  $v_p$  known as  $U-u$  Hugoniot, where  $U$  and  $u$  correspond to shock and particle velocities and  $m$  is the slope of this Hugoniot [17]. Shock data for the liner materials and RHA are listed in Table 2.

**Table 2.** Material properties

Material	Density [g/cm <sup>3</sup> ]	CI [m/s]	Gruneisen coefficient	Slope	Ref.
Aluminium	2.710	5380	2.10	1.337	[18]
Teflon	2.153	1841	0.59	1.707	[19]
Epoxy	1.186	2730	1.13	1.493	
Perspex	1.186	2598	0.97	1.516	[20]
RHA	7.860	4610	1.67	1.730	[18]

Two angles of attack *viz.* 90° and 30° were chosen for the simulations. The aim of the simulations was to find the velocity of the jet after passing the 15 mm thick RHA plate. The decrease in the angle of attack from 90° to 30° caused a 15 mm increase in the target's effective thickness. Therefore two distinct liners of each material were designed for the 90° and 30° attack angles. Direct detonation with the boundary condition of flow out to "ALL EQUAL" was used. The boundary condition directs the software such that once the material moves out of the boundary it does not contribute further to the simulation.

## 2.2 LS Dyna simulations

The second simulation software employed for the design of EFPs was LS Dyna. It is more robust than Autodyn. Two-dimensional axial symmetry, arbitrary Lagrange Eulerian (ALE) solver and the units centimetre, gram and microsecond were utilized. For explosives the JWL, and for other materials the shock equation of state, as mentioned in Equations 1 and 2, were utilized. The material models and equation of states utilized for air, explosives and liners, including RHA, were \*MAT\_NULL, \*MAT\_HIGH\_EXPLOSIVE\_BURN, \*MAT\_ELASTIC\_PLASTIC\_HYDRO, and \*EOS\_LINEAR\_POLYNOMIAL, \*EOS\_JWL, \*EOS\_GRUNEISEN, respectively. No boundary condition is required in LS Dyna.

## 2.3 Experimental technique

An EFP consists of four parts: the casing, liner, lid and explosive. All three metallic components, the casing, lid and liner were manufactured from solid cylindrical rods by lathe turning. The cutting size for the machine during turning of the liner was reduced to give better tolerance control. The casing, after fitting the liner, was preheated before filling with Comp-B. The assembly was then cooled in a controlled manner to avoid porosity in the explosive. The compartment for the initiating explosive/pellet was made within the lid. The lid was closed after placing the tetryl pellets within it. The detonator was added to the assembly after

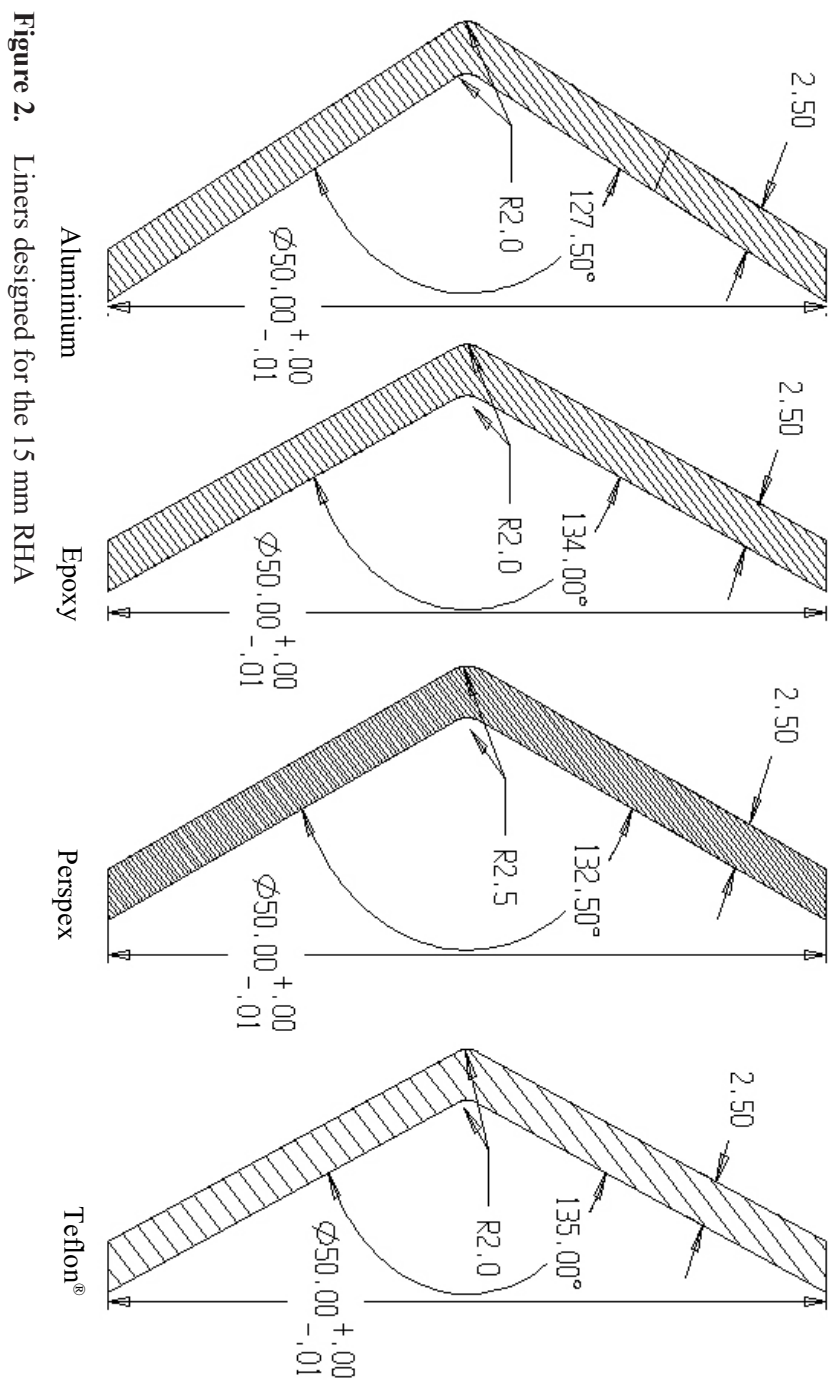
adjusting the angle of attack and stand-off. In the first two experiments, the jets produced by the EFP were radiographed with the flash radiography technique, and showed consistency with the results obtained from Autodyn and LS Dyna.

### 3 Results

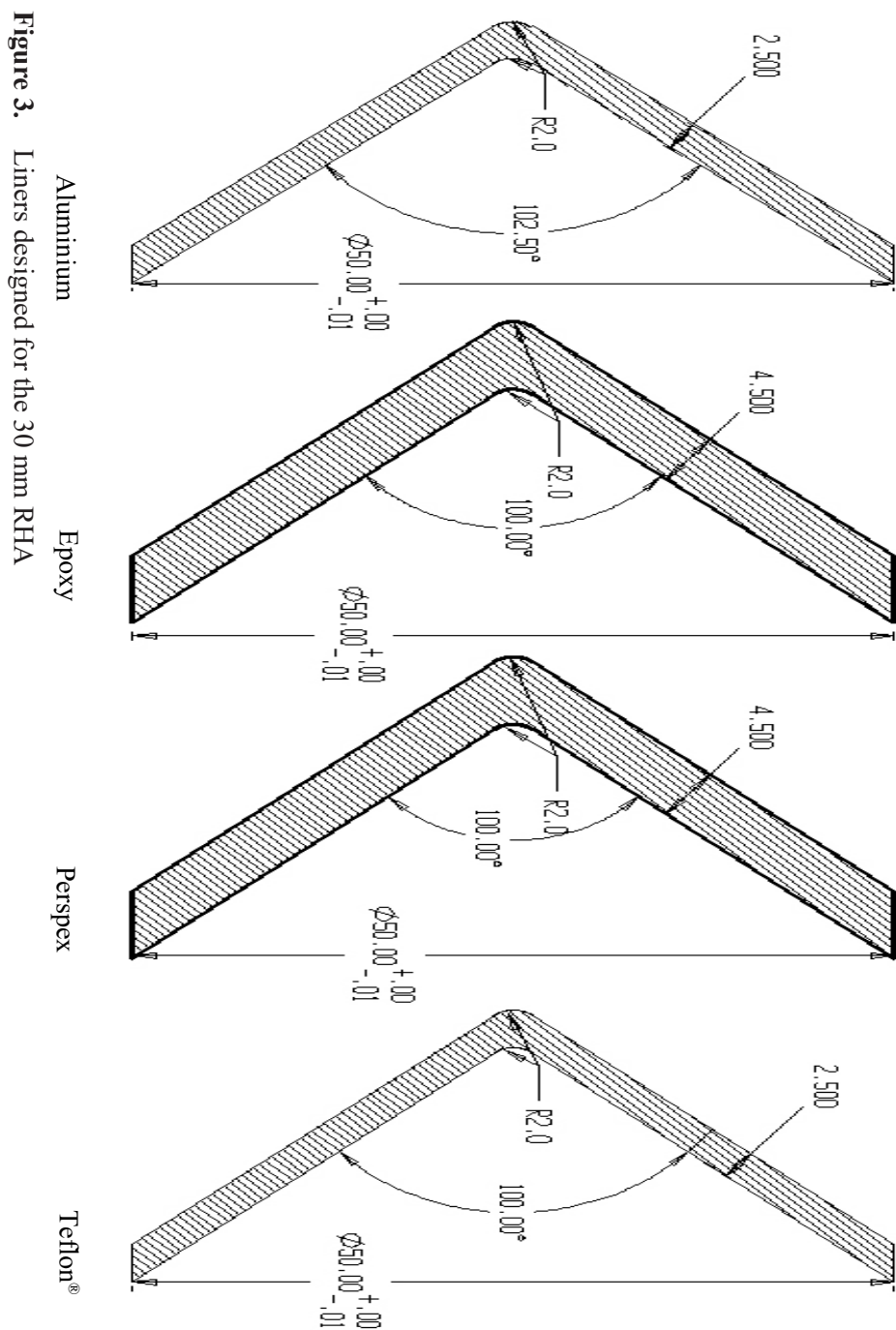
The machine drawings of the liners, finalized after simulation for 15 and 30 mm thick RHAs are shown in Figures 2 and 3, respectively. All of the liners, excluding epoxy, were tested experimentally against the ERA cassettes. This section includes the experimental results from the eight experiments performed on the interaction of the EFP and the ERA at 90° and 30° angles of attack. Comp-B with a density of  $1.71 \pm 0.01$  g/cm<sup>3</sup> was melt-cast as the main charge for the EFP. The results are listed in Table 3, and the diameter of the holes observed in the experiments and simulations are plotted in Figure 4. The term “M/C” is the ratio of the liner to explosive mass. The photographs of the experiments are shown in Figure 5.

**Table 3.** Various parameters and results of the experiments

Experiment No	Liner material	Design and manufactured angle [°]	Liner mass [g]	Mass to charge ratio	Attack angle [°]	RHA effective thickness [mm]	Observation
3	Perspex	132.5, 132.64	5	0.038	90	15	Detonation
4	Teflon®	135, 134.5	11.6	0.09	80	15.23	Detonation
5		135, 135.32	11.5	0.09	40	23.33	Perforation
6	Perspex	132.5, 132.64	5	0.04	45	21.21	No Detonation
7	Aluminium	127.5, 127.43	11.7	0.09	45	21.21	Perforation
8	Teflon®	100, 100.38	11.6	0.09	29.8	30.18	Perforation
9	Aluminium	102.5, 102.53	10.5	0.08	30.1	29.91	Detonation
10	Perspex	100, 100.58	13.7	0.11	29.8	30.18	Perforation



**Figure 2.** Liners designed for the 15 mm RHA





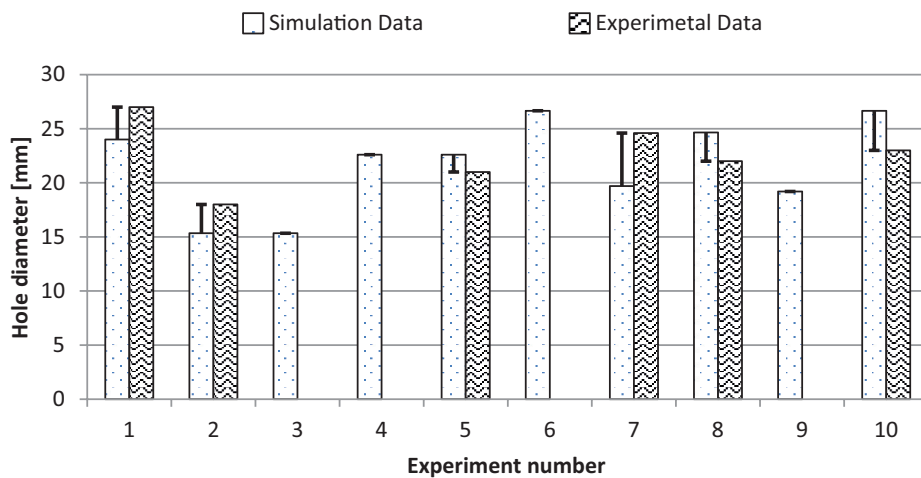


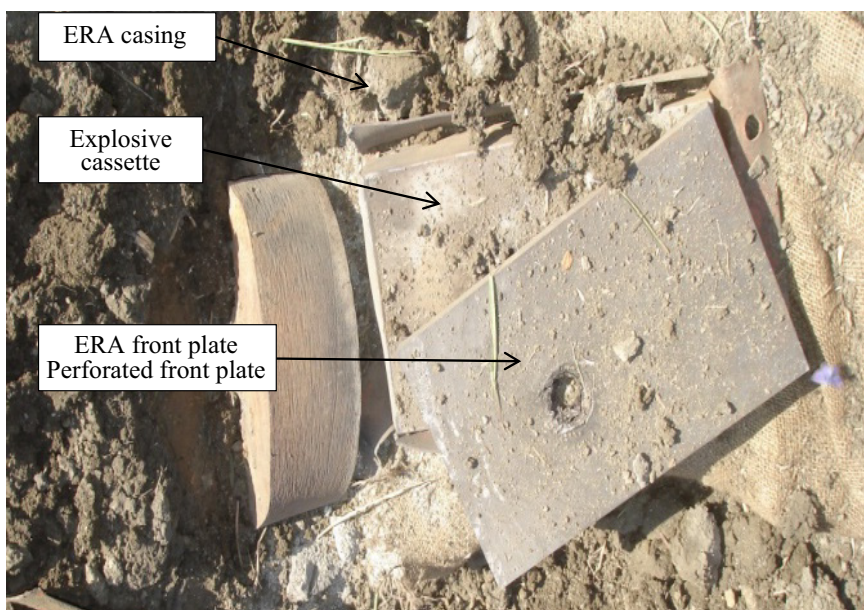
**Figure 4.** Comparison of experimental and simulation hole diameters



(a)



(b)



(c)



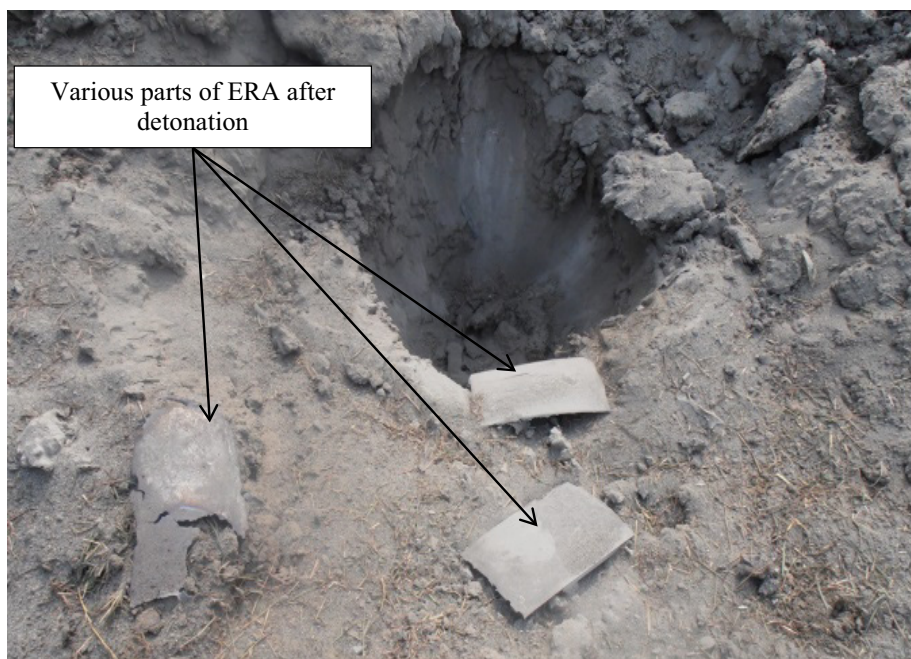
(d)



(e)



(f)



(g)



(h)

**Figure 5.** Pictorial summary of the experiments, No.: (a) 3, (b) 4, (c) 5, (d) 6, (e) 7, (f) 8, (g) 9, and (h) 10

## 4 Discussion

The detonation was observed in experiment 3, where the angle of attack was  $90^\circ$ . In the next experiment the effective thickness was increased by changing the angle of attack to  $80^\circ$ , but this increase was not enough and the jet still had sufficient energy to detonate the explosive within the ERA. Experiment 5 was a complete success. In this experiment, the angle of attack was changed to  $40^\circ$  so the jet had to pass a greater thickness before hitting the explosive cassette. During its passage, the jet gradually lost energy within the front plate of the ERA and hit the explosive cassette with energy less than that required for initiation, as per the “ $v^2d$ ” criterion of detonation as given in Figure 1. In experiment 6, a perspex liner was fired where the effective thickness of the front plate was 21.2 mm. This time the jet was unable to perforate the front plate and produced a dent. During its transit within the front plate the jet interacted with the front plate causing it to lose energy. As the liner was only 5 g in mass, there was insufficient matter available for the jet. Therefore the jet finally came to a halt after losing all its energy without perforation. Thus a lower liner mass,

as given in Table 3, is one of the reasons for no perforation. The other reason was that the EFP designed for a 15 mm thickness was fired at an effective thickness of 21.2 mm. In experiment 7, the aluminium liner was able to perforate the ERA front plate but it caused burning of the ERA. The ERA burnt because it had been used earlier in experiment 6, where it absorbed a sufficient amount of energy. Experiments 8, 9 and 10 were performed at 30° angle of attack, where the effective thickness of the front plate becomes twice its actual thickness. In experiments 8 and 10 the ERA was perfectly neutralized by the NIP but in experiment 9 the ERA detonated. The reasons for detonation in these three experiments may be as described below.

The explosive-fill in the ERA cassette was a mixture of RDX and hydroxyl-terminated polybutadiene (HTPB) in the ratio of 90:10. The mixture was made by hand, therefore there is a chance for inhomogeneity in the explosive making it more sensitive, and resulted in the detonation of the ERA. There was a small variation in the designed and the manufactured angle of the liner. As the liner apex angle is a critical factor in controlling the velocity and shape of the jet, these two are the deciding factors for the initiation of explosives as mentioned in the “ $v^2d$ ” criterion. Therefore a small deviation in the apex angle can produce unwanted effects like detonation.

In all of the experiments the jet over-performed, which was balanced by increasing the effective thickness of the front plate, but in these experiments the over-performance was not completely balanced.

A comparison of the hole diameter produced in the Autodyn simulation and in the experiments is presented in Figure 5. As a whole, no detonation was witnessed in five out of eight experiments. The percentage success could be further enhanced by preparing a homogeneous explosive for the ERA cassette and controlling the tolerance in the manufacturing process, especially in the liners.

## 5 Conclusions

- ◆ All of the experiments were conducted successfully. The ERA was neutralized successfully in five experiments whereas detonation was witnessed in experiments 3, 4 and 9 only. One cause of the detonation may be inhomogeneity in the explosive cassette of the ERA, which makes it more sensitive. The inhomogeneity of the explosive may arise due to hand mixing of RDX and HTPB. Another reason may be the deviation in the designed and manufactured apex angle of the liner as listed in Table 3.

- ◆ In experiments 5, 8 and 10 the hole produced by the NIP had a smaller diameter than predicted by the simulations. This occurred because the NIP in these experiments was aimed at the ERA at an angle greater than the designed one, resulting in an increased effective thickness of the ERA front plate.
- ◆ No detonation was witnessed in experiment 6, only a dent/bulge was produced. This occurred because the EFP was designed for a 15 mm thickness, but was fired at an effective thickness of 21.2 mm. The ERA cassette which did not perforate in experiment 6 was reused in experiment 7, but was aimed some distance away from the bulge and produced a hole larger in diameter than predicted by the simulation. The EFP over-performed in experiments 1 and 2, as is clear from Figure 5. The reason for a larger hole in experiment 7 may be the brittleness of the ERA front plate caused by its earlier utilization in experiment 6. As a whole, seven out of ten experiments gave their desired results. The NIP in all cases over-performed and was aimed at an effective thickness greater than the designed one. The percentage success could be further enhanced by reducing the tolerance in the manufacturing process, especially in making the liners.
- ◆ The overall conclusion of this work is that an NIP is a promising technique to defeat a specific ERA without detonation

## References

- [1] Medin, G.; Olsson, E.; Lennart, S.; Lundgren, R. *Reactive Armor Wall Structure*. Patent US 5012721, **1991**.
- [2] Held, M. Analytical Initiation Criteria of High Explosives at Different Projectile or Jet Densities. *AIP Conf. Proc.* **1996**, pp. 867-870.
- [3] Shin, H.; Lee, W. A Numerical Study on the Detonation Behaviour of Double Reactive Cassettes by Impacts of Projectiles with Different Nose Shapes. *Int. J. Impact Eng.* **2003**, 28(4): 349-362.
- [4] Wiśniewski, A.; Podgórzak, P. Research Results on Precursor of the Tandem Shaped Charge Projectile Model. *Issues Armament Technol. (Problemy Techniki Uzbrojenia)* **2005**, 34(94): 31-38.
- [5] Held, M. Shaped Charge Optimisation Against Bulging Targets. *Propellants Explos., Pyrotech.* **2005**, 30(5): 363-368.
- [6] Held, M. Momentum Theory of Explosive Reactive Armours. *Propellants Explos., Pyrotech.* **2001**, 26(2): 91-96.
- [7] Wiśniewski, A. Explosive Sensitivity Influence on One- and Two-Layered Reactive Armours' Behavior. *J. Appl. Mech.* **2010**, 77(5) paper 051901: 1-9.
- [8] Helte, A.; Lundgren, J. Non-initiating Precursor Charge Technology Against ERA.

- Proc. 26<sup>th</sup> Int. Symp. On Ballistics* **2011**, 313-318.
- [9] Trzciński, W.A.; Cudziło, S.; Dyjak, S.; Szymańczyk, L. Experimental and Theoretical Investigation of a Model Reactive Armour with Nitrocellulose and Cellulose Composite. *Cent. Eur. J. Energ. Mater.* **2013**, *10*(2): 191-207.
- [10] Micković, D.; Jaramaz, S.; Elek, P.; Miloradović, N.; Jaramaz, D. A Model for Explosive Reactive Armor Interaction with Shaped Charge Jet. *Propellants Explos., Pyrotech.* **2016**, *41*(1): 53-61.
- [11] Rasheed, M.F.; Cheng, W.; Raza, A.; Zakir, S.M. Analysis of EFP and Single Sandwitch ERA Interaction. *Proc. 13<sup>th</sup> Int. Bhurban Conf. on Applied Sciences and Technology (IBCAST)*, **2016**, pp. 1-6.
- [12] Bouvenot, F. *The Legacy of Manfred Held with Critique*. Naval Postgraduate School, Dept. of Physics, Monterey, US, **2011**.
- [13] Ding, L.; Tang, W.; Ran, X. Simulation Study on Jet Formability and Damage Characteristics of a Low-Density Material Liner. *Materials* **2018**, *11*(72): 1-17.
- [14] Rasheed, M.F.; Wu, C.; Raza, A. Effect of Explosive Reactive Armour Cover Plate on Interaction of ERA and Explosively Formed Projectile. *Shock Vib.* **2019**, paper 6093621: 1-10.
- [15] Nacem, K.; Hussain, A. Numerical and Experimental Study of Wave Shaper Effects on Detonation Wave Front. *Def. Technol.* **2017**, *14*(1): 45-50.
- [16] Lee, E.; Finger, M.; Collins, W. *JWL Equation of State Coefficients for High Explosives*. Lawrence Livermore National Lab. Report UCID-16189, Livermore, CA, US, **1973**.
- [17] Cooper, P.W. *Explosives Engineering*. 1<sup>st</sup> ed., Wiley VCH Pub., USA, **1996**; ISBN 0471186368.
- [18] Matuska, D. *HULL user's manual*. AFATL-TR-84-59, **1984**.
- [19] *AUTODYN – A Material Library*. **2016**.
- [20] Stirpe, D.; Johnson, J.O.; Wackerle, J. *Selected Hugoniot. Group GMX-6*. Los Alamos National. Lab., Report LA-4167-MS, **1969**.

Received: September 8, 2020

Revised: June 29, 2021

First published online: June 30, 2021